

PHASE RELATIONS IN THE  $\text{Tl}_5\text{Te}_3$ - $\text{Tl}_9\text{SbTe}_6$ - $\text{Tl}_9\text{TbTe}_6$  SYSTEM

*Samira Imamaliyeva*<sup>1, \*</sup>, *Turan Gasanly*<sup>2</sup>, *Imameddin Amiraslanov*<sup>3</sup>,  
*Mahammad Babanly*<sup>1</sup>

https

**Abstract.** Phase relations in the  $\text{Tl}_5\text{Te}_3$ - $\text{Tl}_9\text{SbTe}_6$ - $\text{Tl}_9\text{TbTe}_6$  system were experimentally studied by DTA, XRD technique and microhardness measurements. Several isopleth sections and isothermal section at 760 K, as well as projections of the liquidus and solidus surfaces were constructed. It is determined that the system is characterized by an unlimited solubility of components in the solid state.

**Keywords:** thallium-therbium tellurides, thallium-antimony tellurides, phase relations, projections of the liquidus, solid solutions, crystal structure.

## 1. Introduction

Chalcogenides of heavy *p*-elements are essential due to their important properties like thermoelectric, optical, *etc.* [1-3]. Moreover, some of such compounds have attracted scientific and technological interest as topological insulators [4, 5].

Rare earth elements tellurides are important materials for the fabrication of microbatteries, multilayer high-efficiency solar cells, *etc.* [6]. Moreover, *ab-initio* calculations [7] shown that  $\text{LaBiTe}_3$  is a topological insulator and exhibits thermoelectric properties [8].

Thallium subtelluride,  $\text{Tl}_5\text{Te}_3$ , due to features of its crystal structure is suitable “matrix” for fabrication of novel complex materials. This compound crystallizes in tetragonal structure [9] (Sp.gr. I4/mcm,  $a = 8.930$ ;  $c = 12.598$  Å) with four formula units per unit cell (Fig. 1). The basic structural component of  $\text{Tl}_5\text{Te}_3$  compound is octahedron with a thallium atom, Tl(2), in its center. These octahedra connected by vertices form a frame

$\text{Tl}_4\text{Te}_{12}$ , or  $(\text{TlTe}_3)_4$ . The other 16 thallium atoms, Tl(1) link octahedra along the *c* axis and form a unit cell  $\text{Tl}_{16}(\text{TlTe}_3)_4$ .  $\text{B}^{3+}$  ( $\text{B}^{3+}$ -Sb, Bi) substitution for half of the Tl(2) atoms, resulting in the compounds  $\text{Tl}_9\text{BTe}_6$  or  $\text{Tl}_{16}[(\text{Tl}_{0.5}^{1+}\text{B}_{0.5}^{3+})\text{Te}_3]_4$  (I), while the replacement of all these thallium atoms by cations  $\text{A}^{2+}$  ( $\text{A}^{2+}$ -Sn, Pb) is leading to formation of  $\text{Tl}_4\text{ATE}_3$  or  $\text{Tl}_{16}[\text{A}^{2+}\text{Te}_3]_4$  (II).

Compounds of type (I) and (II) were detected during the experimental phase relations investigations of respective ternary systems [10-13]. These materials have good thermoelectric performance, whereas  $\text{Tl}_9\text{BiTe}_6$  was found to have the highest ZT value ( $\text{ZT} = 1.2$  at 500 K) [14-16]. Furthermore, authors [17] report the discovery of Dirac-like surface states in  $[\text{Tl}_4](\text{Tl}_{1-x}\text{Sn}_x)\text{Te}_3$  and  $\text{Tl}_5\text{Te}_3$ .

Earlier we presented new thallium lanthanide tellurides with composition  $\text{Tl}_9\text{LnTe}_6$  (Ln-Ce, Nd, Sm, Gd, Tm, Tb), which were found to be ternary substitution variant of  $\text{Tl}_5\text{Te}_3$  [18-20]. Moreover, it was shown that ytterbium does not form the compound  $\text{Tl}_9\text{YbTe}_6$  [20, 21]. Latter, H. Kleinke *et al.* determined the crystal structure as well as magnetic and thermoelectric properties for a number of  $\text{Tl}_9\text{LnTe}_6$ -type compounds [22-25].

In order to obtain solid solutions based on  $\text{Tl}_5\text{Te}_3$ -potential thermoelectric material, we investigated phase equilibria of a number of systems including  $\text{Tl}_5\text{Te}_3$  compound or its structural analogues [26-28]. We found that these systems are characterized by formation of continuous solid solutions.

The investigation performed in the present paper is aimed to study phase relations in the  $\text{Tl}_5\text{Te}_3$ - $\text{Tl}_9\text{SbTe}_6$ - $\text{Tl}_9\text{TbTe}_6$  system.

Starting compounds are well known materials.  $\text{Tl}_5\text{Te}_3$  and  $\text{Tl}_9\text{SbTe}_6$  melt congruently at 723 K [29] and 800 K [10] while  $\text{Tl}_9\text{TbTe}_6$  melts with decomposition by the peritectic reaction at 780 K [30]. The lattice parameters of  $\text{Tl}_9\text{TbTe}_6$  and  $\text{Tl}_9\text{SbTe}_6$  are the following:  $a = 8.871$ ,  $c = 12.973$ ,  $z = 2$  [30];  $a = 8.829$ ,  $c = 13.001$  Å,  $z = 2$  [31].

According to the phase diagram of the  $\text{Tl}_5\text{Te}_3$ - $\text{Tl}_9\text{SbTe}_6$  system, this system is characterized by formation of continuous solid solution field with  $\text{Tl}_5\text{Te}_3$ -type structure [10].

<sup>1</sup> Institute of Catalysis and Inorganic Chemistry named after acad. M. Nagiyev, Azerbaijan National Academy of Sciences, 113 H.Javid Ave., Az-1143, Baku, Azerbaijan

<sup>2</sup> Baku State University, 23 Z.Khalilov St., 23, Az-1148, Baku, Azerbaijan

<sup>3</sup> Institute of Physics, Azerbaijan National Academy of Sciences, 131 H.Javid Ave., Az1143, Baku, Azerbaijan

\* [samira9597a@gmail.com](mailto:samira9597a@gmail.com)

© Imamaliyeva S., Gasanly T., Amiraslanov I., Babanly M., 2017

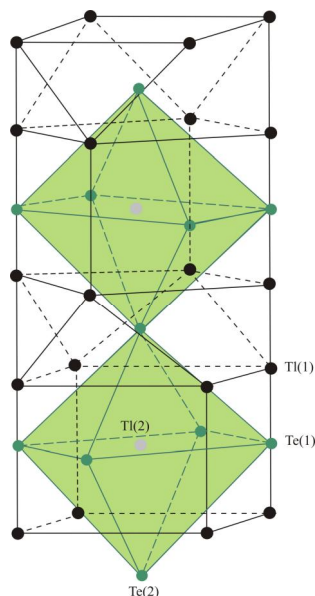


Fig. 1. Basic structural component of  $Tl_5Te_3$  compound

## 2. Experimental

### 2.1. Materials and Syntheses

Thallium (granules, 99.999 %), antimony (granules, 99.999 %), terbium (powder, 99.9 %), and tellurium (broken ingots 99.999 %) were used as starting components. The surface of thallium was covered by oxide film, which was removed before use.

These starting materials were weighed in proper molar ratio of the corresponding compound and put into silica tubes of about 20 cm in length and then were sealed under a vacuum of  $10^{-2}$  Pa.

The synthesis of  $Tl_5Te_3$  and  $Tl_9SbTe_6$  compounds was carried out by heating in one-zone electric furnace at the 30-50° above the melting point of the compounds followed by cooling in the switched-off furnace.

Taking into account the results of [30, 32], the obtained intermediate ingot of  $Tl_9TbTe_6$  was carefully powdered in agate mortar, pressed into pellet and annealed at 750 K within ~1000 h. In order to avoid reaction between the terbium and the silica ampoule, a thin layer of carbon was deposited on the inner side of quartz tube by the pyrolysis of acetone.

The purity of the synthesized starting compounds was checked by the differential thermal analysis (DTA) and X-ray diffraction (XRD).

Only one endothermic effect was observed for  $Tl_5Te_3$  (723 K) and  $Tl_9SbTe_6$  (790 K) while two effects for  $Tl_9TbTe_6$  (780 and 1110 K) showed the completion of the synthesis.

Powder XRD pattern of the  $Tl_9SbTe_6$  and  $Tl_9TbTe_6$  were same as that of  $Tl_5Te_3$ . Their unit cell lattice parameters were practically equal with the [30, 31] (see Table).

The alloys of the  $Tl_5Te_3$ - $Tl_9SbTe_6$ - $Tl_9TbTe_6$  system were prepared by melting from pre-synthesized compounds in evacuated silica ampoules. Taking into account the fact that an equilibrium state could not be obtained even after the long-time (1000 h) annealing [30, 32], after synthesis the samples were powdered, mixed, pressed into pellets and annealed at 700 K for ~800 h.

### 2.2. Methods

The samples were analyzed by X-ray diffraction and differential thermal analysis as well as microhardness measurements.

The XRD measurements of powdered specimen were recorded using a Bruker D8 diffractometer utilizing  $CuK_{\alpha}$  radiation within  $2\theta = 10-70^{\circ}$ . DTA was performed using a NETZSCH 404 F1 Pegasus differential scanning calorimeter within room temperature and ~1400 K at the heating rate of  $10 K \cdot min^{-1}$ . Microhardness measurements were done with a microhardnesmeter PMT-3, the typical loading being 20 g.

## 3. Results and Discussion

The combined analysis of experimental and literature data [10, 29, 30] enabled to construct the self-consistent diagram of the phase relations in the  $Tl_5Te_3$ - $Tl_9BiTe_6$ - $Tl_9TbTe_6$  system (Table, Figs. 2-7).

The equilibrium phase diagrams of the  $2Tl_5Te_3$ - $Tl_9TbTe_6$  and  $Tl_9SbTe_6$ - $Tl_9TbTe_6$  system (Figs. 2a and 3a) are characterized by the formation of a continuous solid solutions (*d*) with  $Tl_5Te_3$ -type structure. However, these systems are non-quasi-binary due to peritectic melting of  $Tl_9TbTe_6$ . This leads to crystallization of unknown infusible X phase (presumably  $TlTbTe_2$ ) in a wide composition range and formation of L+X and L+X+*d* phase areas. However, these areas are not experimentally fixed due to narrow temperature interval and shown by dashed line.

Microhardness measurements are in good agreement with *T-x* phase diagram (Figs. 2b and 3b): curves have a flat maximum (Figs. 2b and 3b), which is typical for systems with continuous solid solutions.

The formation of continuous solid solutions in the studied systems is confirmed by XRD (Fig. 4). Apparently, powder diffraction patterns of starting compounds and intermediate alloys were same as that of  $Tl_5Te_3$  with slight reflections displacement from one compound to another. The lattice parameters of solid solutions obey the Vegard's law, *i.e.* depend linearly on composition.

Some properties of phases in the  $Tl_5Te_3$ - $Tl_9SbTe_6$ - $Tl_9TbTe_6$  system

Phase	Temperature of melting, K	Microhardness, MPa	Parameters of tetragonal lattice, Å	
			<i>a</i>	<i>c</i>
$Tl_5Te_3$	723	1130	8.930	12.598
$Tl_{9.9}Tb_{0.1}Te_6$	730	—	—	—
$Tl_{9.8}Tb_{0.2}Te_6$	735–742	1160	8.918	12.681
$Tl_{9.6}Tb_{0.4}Te_6$	740–756	1140	8.907	12.761
$Tl_{9.4}Tb_{0.6}Te_6$	750–763	1120	8.895	12.842
$Tl_{9.2}Tb_{0.8}Te_6$	763–775; 1045	1070	8.883	12.919
$Tl_{9.1}Tb_{0.9}Te_6$	770–778	—	—	—
$Tl_9TbTe_6$	780; 1110	1100	8.871(9)	12.973(3)
$Tl_9Sb_{0.1}Tb_{0.9}Te_6$	781; 1080	—	—	—
$Tl_9Sb_{0.2}Tb_{0.8}Te_6$	782	1160	8.8626	12.9786
$Tl_9Sb_{0.4}Tb_{0.6}Te_6$	783–785	1140	8.8542	12.9842
$Tl_9Sb_{0.5}Tb_{0.5}Te_6$	784–786	—	—	—
$Tl_9Sb_{0.6}Tb_{0.4}Te_6$	785–787; 1030	1130	8.8458	12.9898
$Tl_9Sb_{0.8}Tb_{0.2}Te_6$	788	1080	8.8374	12.9954
$Tl_9SbTe_6$	790	1000	8.8312(2)	13.0132(1)

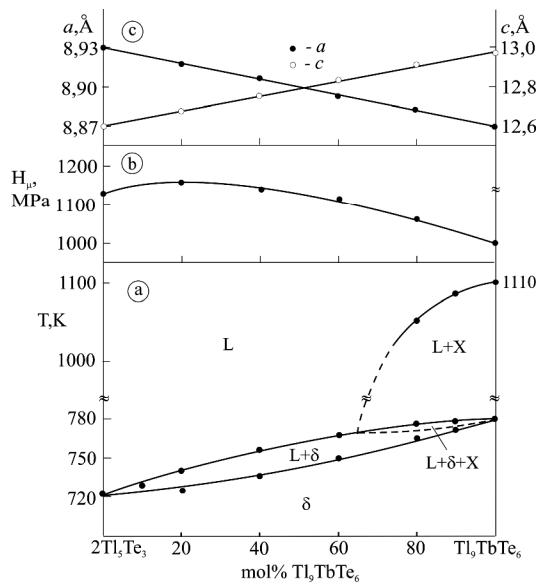


**Fig. 2.** Phase diagram (a), concentration relations of microhardness (b), and lattice parameters (c) for the system  $2Tl_5Te_3$ - $Tl_9TbTe_6$

**The liquidus surface projection (Fig. 5).** Liquidus of  $Tl_5Te_3$ - $Tl_9SbTe_6$ - $Tl_9TbTe_6$  system consists of two fields of the primary crystallization of X-phase and *d*-solid solutions. These fields are separated by *ab* curve that corresponds to the monovariant peritectic equilibrium  $L+X \leftrightarrow d$ .

**Isopleth sections of the  $Tl_5Te_3$ - $Tl_9SbTe_6$ - $Tl_9TbTe_6$  system (Fig. 6).** Figs. 6a-c show the isopleth sections  $2Tl_5Te_3$ -[C],  $Tl_9SbTe_6$ -[A] and  $Tl_9TbTe_6$ -[B] of the  $Tl_5Te_3$ - $Tl_9SbTe_6$ - $Tl_9TbTe_6$  system, where A, B and C are alloys from the respective boundary system.

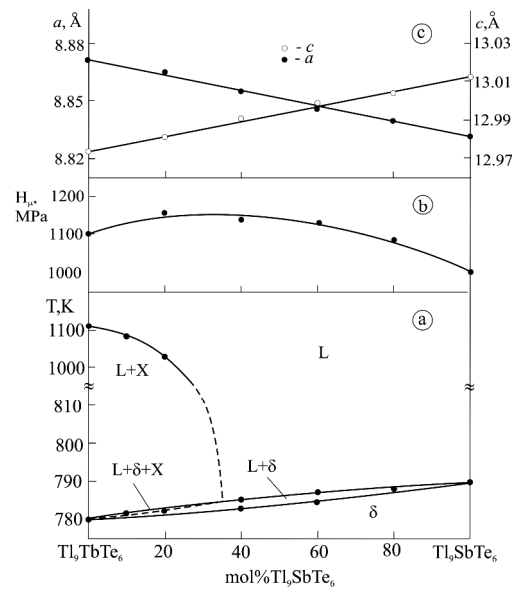


**Fig. 3.** Phase diagram (a), concentration relations of microhardness (b), and lattice parameters (c) for the system  $Tl_9TbTe_6$ - $Tl_9SbTe_6$

As can be seen, over the entire compositions range of the  $Tl_9SbTe_6$ -[A] и  $Tl_5Te_3$ -[C] systems only *d*-phase crystallizes from the melt.

According to the phase diagram of the  $Tl_9TbTe_6$ -[B] section, in the composition area  $<60$  mol %  $Tl_9TbTe_6$  the primary crystallization of the *d*-phase occurs from the liquid phase. In the  $Tl_9TbTe_6$ -rich alloys the X-phase first crystallizes, then a monovariant peritectic equilibrium  $L+X \leftrightarrow d$  takes place.

It should be noted that conode positions in two-phase area  $L+d$  do not correspond to the cross section planes and continuously change with temperature. The conode positions at 760 K are shown in Fig. 7.

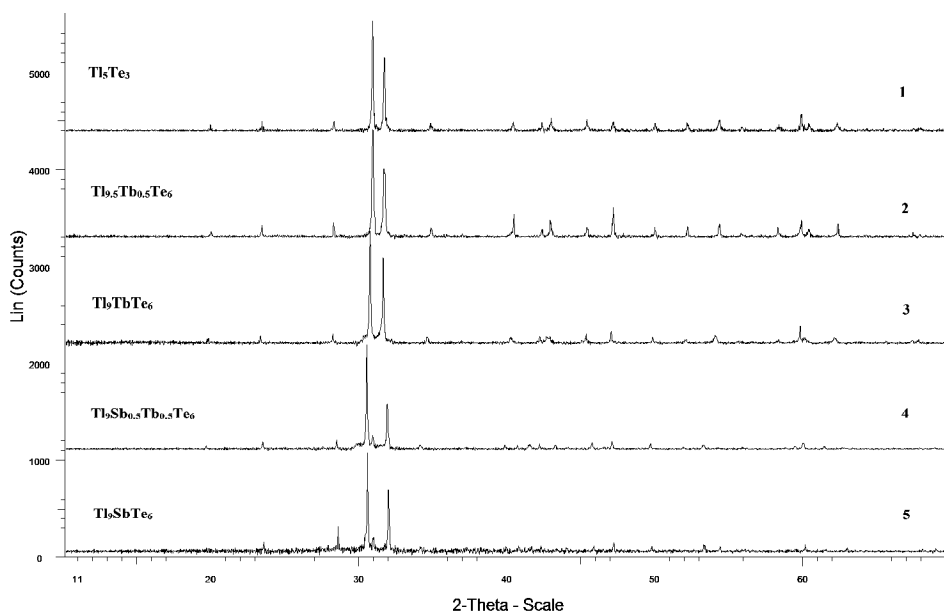


**Fig. 4.** XRD patterns for different compositions in the  $Tl_5Te_3$ - $Tl_9TbTe_6$  (patterns 1-3) and  $Tl_9TbTe_6$ - $Tl_9SbTe_6$  (patterns 3-5) systems:  $Tl_5Te_3$  (1); 50 mol %  $Tl_9TbTe_6$  (2);  $Tl_9TbTe_6$  (3); 50 mol %  $Tl_9TbTe_6$  (4) and  $Tl_9SbTe_6$  (5)

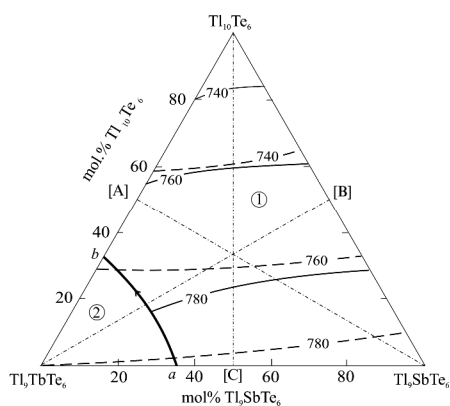


**Fig. 5.** Projection of the liquidus and solidus (dashed lines) surface of the  $Tl_5Te_3$ - $Tl_9TbTe_6$ - $Tl_9SbTe_6$  system:  $d$  (1) and X phase (2). Dash-dot lines show the investigated sections

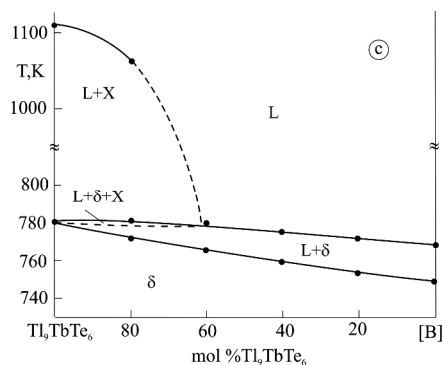
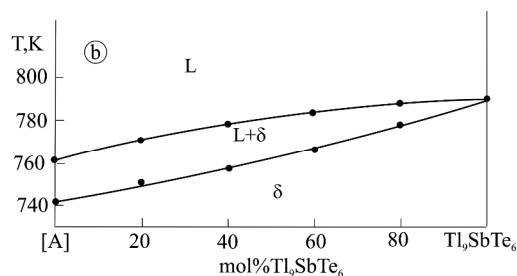
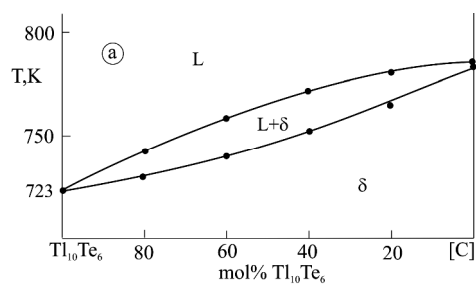


**Fig. 6.** Polythermal sections  $Tl_{10}Te_6$ -[C],  $Tl_9SbTe_6$ -[A] and  $Tl_9TbTe_6$ -[B] of the phase diagram of the  $Tl_5Te_3$ - $Tl_9TbTe_6$ - $Tl_9SbTe_6$  system

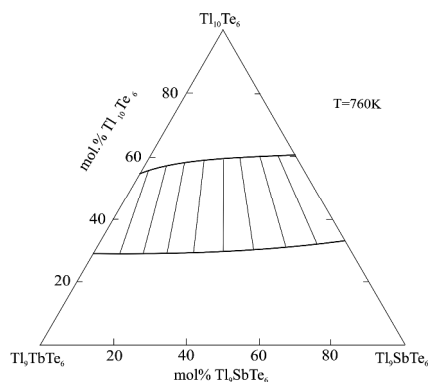


**Fig. 7.** Isothermal section of the phase diagram of the  $Tl_5Te_3$ - $Tl_9TbTe_6$ - $Tl_9SbTe_6$  system at 760 K

## 4. Conclusions

A complete  $T$ - $x$ - $y$  diagram of the  $Tl_5Te_3$ - $Tl_9SbTe_6$ - $Tl_9TbTe_6$  system, including the  $T$ - $x$  diagrams of boundary systems  $Tl_5Te_3$ - $Tl_9TbTe_6$  and  $Tl_9SbTe_6$ - $Tl_9TbTe_6$ , some isopleth sections, isothermal section at 760 K, as well as the liquidus and solidus surface projections were constructed. It is found that the system is characterized by an unlimited solubility of components in the solid state. The obtained experimental data can be used for the choice of composition of solution-melt and for determining of temperature conditions for growing crystals of  $d$ -phase with a given composition.

## Acknowledgements

The work was supported by the Science Foundation of the State Oil Company of Azerbaijan Republic (Grant for the project "Preparation and investigation of new functional materials based on complex metal chalcogenides for alternative energy sources and electronic engineering", 2014).

## References

- [1] Novoselova A., Lazarev V. (Eds.): Physico-Khimicheskie Svoistva Poluprovodnikovykh Materialov. Nauka, Moskva 1979.
- [2] Rowe D. (Ed.): CRC Handbook of Thermoelectrics. CRC Press, New York 1995.
- [3] Koc H., Simsek S., Mamedov A., Ozbay E.: Ferroelectrics, 2015, **483**, 43. <http://dx.doi.org/10.1080/00150193.2015.1058672>
- [4] Nechaev I., Aguilera I., Renzi V. *et al.*: Phys. Rev. B, 2015, **91**, 245123. <https://doi.org/10.1103/PhysRevB.91.245123>
- [5] Niesner D., Otto S., Hermann V. *et al.*: Phys. Rev. B, 2014, **89**, 081404. <https://doi.org/10.1103/PhysRevB.89.081404>
- [6] Jha A.: Rare Earth Materials: Properties and Applications. CRC Press, New York 2014. <https://doi.org/10.1201/b17045>
- [7] Yan B., Zhang H-J., Liu C-X. *et al.*: Phys. Rev. B, 2010, **82**, 161108(R). <https://doi.org/10.1103/PhysRevB.82.161108>
- [8] Singh N., Schwingenschlogl U.: Phys. Status Solidi RRL, 2014, **8**, 805. <https://doi.org/10.1002/pssr.201409110>
- [9] Schewe I., Bottcher P., Schnering H.: Z. Kristallogr., 1989, **Bd188**, 287. <https://doi.org/10.1524/zkri.1989.188.14.287>
- [10] Babanly M., Akhmadyar A., Kuliev A.: Russ. J. Inorg. Chem., 1985, **30**, 1051.
- [11] Babanly M., Akhmadyar A., Kuliev A.: Russ. J. Inorg. Chem., 1985, **30**, 2356.
- [12] Gotuk A., Babanly M., Kuliev A.: Inorg. Mater., 1979, **15**, 1062.
- [13] Gotuk A., Babanly M., Kuliev A.: Uch. Zap. Azerb. Un-ta, 1978, **3**, 50.
- [14] Guo Q., Chan M., Kuropatwa B., Kleinke H.: J. Appl. Phys., 2014, **116**, 183702. <https://doi.org/10.1063/1.4938058>
- [15] Kuropatwa B., Guo Q., Assoud A., Kleinke H.: Z. Anorg. Allg. Chem., 2014, **640**, 774. <https://doi.org/10.1002/zaac.201300577>
- [16] Wolfing B., Kloc C., Teubner J., Bucher E.: Phys. Rev. Lett., 2001, **86**, 4350. <https://doi.org/10.1103/PhysRevLett.86.4350>
- [17] Arpino K., Wallace D., Nie Y. *et al.*: Phys. Rev. Lett., 2014, **112**, 017002. <https://doi.org/10.1103/PhysRevLett.112.017002>
- [18] Imamaliyeva S., Sadygov F., Babanly M.: Inorg. Mater., 2008, **44**, 935. <https://doi.org/10.1134/S0020168508090070>
- [19] Babanly M., Imamaliyeva S., Babanly D., Sadygov F.: Azerb. Chem. J., 2009, **2**, 121.
- [20] Babanly M., Imamaliyeva S., Sadygov F.: News of BSU. Nat. Sci. Ser., 2009, **4**, 5.
- [21] Imamaliyeva S., Mashadiyeva L., Zlomanov V., Babanly M.: Inorg. Mater., 2015, **51**, 1237. <https://doi.org/10.1134/S0020168515110035>
- [22] Sankar C., Bangarigadu-Sanasy S., Kleinke H.: J. Elec. Mater., 2012, **41**, 1662. <https://doi.org/10.1007/s11664-011-1846-z>
- [23] Bangarigadu-Sanasy S., Sankar C., Schlender P., Kleinke H.: J. Alloy. Compd., 2013, **549**, 126. <https://doi.org/10.1016/j.jallcom.2012.09.023>
- [24] Bangarigadu-Sanasy S., Sankar C., Dube P. *et al.*: J. Alloy. Compd., 2014, **589**, 389. <https://doi.org/10.1016/j.jallcom.2013.11.229>
- [25] Guo Q., Kleinke H.: J. Alloy. Compd., 2015, **630**, 37. <https://doi.org/10.1016/j.jallcom.2015.01.025>
- [26] Babanly M., Tedenac J.-C., Imamaliyeva S. *et al.*: J. Alloy. Compd., 2010, **491**, 230. <https://doi.org/10.1016/j.jallcom.2009.08.157>
- [27] Imamaliyeva S., Guseynov F., Babanly M.: Chem. Probl. J., 2008, **4**, 640.
- [28] Imamaliyeva S., Guseynov F., Babanly M.: Azerb. Chem. J., 2009, **1**, 49.
- [29] Asadov M., Babanly M., Kuliev A.: Inorg. Mater., 1977, **13**, 1407.
- [30] Imamaliyeva S., Gasanly T., Sadygov F., Babanly M.: Azerb. Chem. J., 2015, **3**, 93.
- [31] Bottcher P., Doert Th., Druska Ch., Bradtmoller S.: J. Alloy. Compd., 1997, **246**, 209. [https://doi.org/10.1016/S0925-8388\(96\)02455-3](https://doi.org/10.1016/S0925-8388(96)02455-3)
- [32] Imamaliyeva S., Gasanly T., Amiraslanov I., Babanly M.: Am. Chem. J., 2016, **10**, 1. <https://doi.org/10.9734/ACSJ/2016/22221>

Received: September 20, 2016 / Revised: October 1, 2016 / Accepted: December 28, 2016

## ФАЗОВІ ВЗАЄМОДІЇ У СИСТЕМІ $Tl_5Te_3$ - $Tl_9SbTe_6$ - $Tl_9TbTe_6$

**Анотація.** За допомогою ДТА і РСА аналізів та вимірювання мікротвердості експериментально вивчені фазові взаємодії в системі  $Tl_5Te_3$ - $Tl_9SbTe_6$ - $Tl_9TbTe_6$ . Побудовані ізоплетний та ізотермічний переріз за 760 К, а також проекції ліквідусу і солідусу поверхонь. Встановлено, що система характеризується необмеженою розчинністю компонентів в твердому стані.

**Ключові слова:** талій-тербій теллуриди, талій-сурма теллуриди, фазова взаємодія, проекції ліквідусу, твердий розчин, кристалічна структура.